J Mol Model (2007) 13: 47–53
DOI 10.1007/s00894-006-0128-9

ORIGINAL PAPER

Craig A. Bayse · Benjamin D. Allison

Activation energies of selenoxide elimination from Se-substituted selenocysteine

Received: 30 March 2006 / Accepted: 4 May 2006 / Published online: 25 May 2006

Abstract Transition states for selenoxide elimination have been determined for a series of Se-substituted selenocysteine (RSeCys) derivatives that have potential use in the prevention and treatment of cancer, either directly or in conjunction with cisplatin (to reduce its nephrotoxic effects). Reduced activation barriers vs R=Me and R=Ph are found when the alkyl chain length is increased or when activating groups are *para* to the selenide. *Ortho* substitution of Lewis bases stabilizes the transition state by directly donating electron density to the selenoxide. The results suggest that RSeCys derivatives incorporating the properties of glutathione peroxidase mimics will, upon oxidation, rapidly eliminate selenenic acid, a precursor to chemopreventative selenols.

Keywords Density functional theory · Selenium · Glutathione peroxidase · Activation energies

Introduction

Naturally occurring methylselenocysteine and selenomethionine are sources of methylselenol, which inhibits tumor growth and induces apoptosis [1]. Other selenols have similar effects; dietary supplementation of *p*-methoxyphenylselenol inhibits carcinogenesis in the colon, kidney, and blood [2]. As a result, significant effort has been invested in the design and delivery of highly active selenols [3]. Vermeulen has proposed Se-substituted selenocysteine derivatives (RSeCys) as a means of targeting selenols to the kidney [4–8]. Both normal and cancerous renal cells contain high levels of β-lyase enzymes, which convert selenides RSeCys to selenols through β-elimination (Scheme 1). Musaev has used density functional theory (DFT) to show that interactions with phosphate groups in the active sites of β-lyase enzymes reduce the barrier for β-elimination [9]. The by-product dehydroglycine is hydrolyzed into ammonia and pyruvate, the latter of which is used to monitor progress of the reaction.

Further experimentation showed that inhibition of β-lyase did not completely stop production of pyruvate. Subsequently, Rooseboom et al. [11] proved that oxidation of RSeCys by flavin-containing monooxygenases produced selenoxides, which can undergo an elimination pathway to produce pyruvate (Scheme 1). However, it is not clear whether selenoxides or their elimination products (selenenic acids) contribute to the chemopreventative activity of RSeCys [5]. Selenenic acids produced in this mechanism can be converted to selenols by thiol reduction.

Many groups have shown that the GPx-like activity of organoselenium compounds can be increased when nearby nitrogen- or oxygen-containing groups interact with the selenium center [10]. These interactions are often supplied through a pendant group arranged *ortho* to selenium on an aromatic ring. Rooseboom et al. [5, 11] have suggested that RSeCys prodrugs that incorporate the properties of good GPx mimics would allow targeting of highly active selenols to the kidney to destroy tumor cells or protect the organ against the nephrotoxic effects of platinum-based chemotherapeutics [11]. Phadnis and Mugesh [12] recently have synthesized several of these compounds and shown that *ortho* pendant groups prevent air oxidation of RSeCys derivatives. Se···N,O interactions may also serve to increase the rate of selenoxide elimination through stabilization of the transition state. Thus, RSeCys prodrugs incorporating Se···N,O interactions could be both air-stable and rapidly eliminate selenenic acids as precursors to highly active selenols.

Various computational studies have examined the strengths of interactions between Se and N, O and the halides [13]. Additionally, Se···N interactions have been shown to occur in selenomethionine selenoxide [14]. In this study, we will examine the influence of the length of alkyl side chain and phenyl substituent effects upon the barrier to selenoxide elimination of various Se-substituted

C. A. Bayse (✉) · B. D. Allison
Department of Chemistry and Biochemistry,
Old Dominion University,
Hampton Boulevard,
Norfolk, VA 23529, USA
e-mail: cbayse@odu.edu

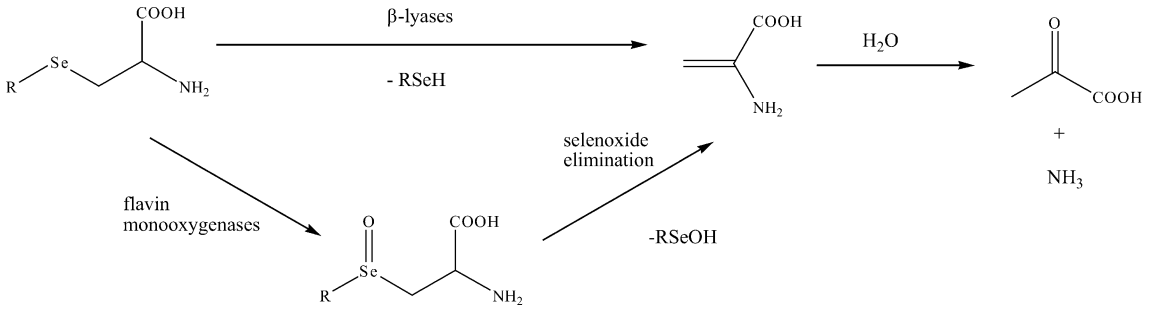

Scheme 1 Elimination pathways for Se-substituted SeCys

SeCys derivatives. We show that *ortho* pendant groups of the kind found in GPx mimics reduce the barrier significantly.

Theoretical methods

Geometry optimizations were performed at the DFT/B3LYP [15] and DFT/mPW1PW91 [16] levels in Gaussian 98 [17]. Selenium was represented by the Hurley et al. [18] relativistic effective core potential double-ζ basis set augmented with even-tempered *s*, *p*, and *d* diffuse functions. Nitrogen and oxygen were represented by Dunning's split-valence triple-ζ plus polarization function basis set [19]. Double-ζ plus polarization basis sets were used for carbon [20]. Basis sets for hydrogen attached to non-carbon heavy atoms were triple-ζ in quality [17], while those for hydrogen attached to carbon were double-ζ [18]. Frequency calculations were used to verify structures as either minima or transition states. Reported energies have been corrected for zero-point energy. Atomic charges were determined by Natural Population Analysis. Donor-acceptor energies $\Delta E_{d\rightarrow a}$, often used in the analysis of nonbonding interactions with Se [11], were calculated using Natural Bond Orbital [21] analysis.

Results and discussion

The mechanism for selenoxide elimination is shown in Scheme 2. The reaction is assumed to proceed through a five-membered transition state consisting of abstraction of the proton from the α carbon (C_α) coupled with cleavage of the Se–C_β bond and formation of a C_α–C_β double bond. Stabilization of positive charge on Se by electron-donating R groups will increase the basicity of O_{SeO}. Electron-withdrawing R groups will pull electron density away from Se, stabilizing the selenoxide bond. An increase in the basicity of the selenoxide oxygen O_{SeO} should result in a lower activation barrier if H abstraction is rate-determining, as in β elimination. Data for the selenoxides and their transition states are summarized in Tables 1 (energetics and partial charges) and 2 (changes in bond lengths between 1 and TS). Energies and parameters resulting from the mPW1PW91 exchange-correlation (XC) functional are listed in the text in parentheses following the B3LYP values. Differences in activation energies and geometric parameters tend to be minimal between these two XC functionals; however, the relative energy of reaction ΔE_{reac} determined by mPW1PW91 is more endothermic by ~5 kcal mol^{-1}.

The high barrier to inversion for the trigonal pyramidal selenium center of 1 imparts chirality to the selenoxide. Coupling the chirality of the selenoxide to that of the α-carbon results in two distinct stereoisomers of 1. Calculations on the *R*- and *S*-selenoxide forms of 1a show that the *S* enantiomer (Fig. 1) is more stable by 0.9 kcal mol^{-1} (B3LYP). This conformation is used throughout this study as the reactant model for larger RSeCys derivatives. Hydrogen-bonding interactions between the selenoxide oxygen and the NH_2 group stabilize both enantiomers, but are artificial to the theoretical gas phase model and may be replaced by interactions with solvent water in solution. The length of this hydrogen bond is a measure of the basicity of the selenoxide oxygen.

The transition state for selenoxide elimination from 1a was optimized in two configurations: Me eclipsed with COOH (TSa) or NH_2 (TSa′). The conformation eclipsed with COOH is associated with selenoxide elimination from the *S*-selenoxide and lies 2.5 kcal mol^{-1} (B3LYP) below TSa′. The activation energy from this conformation is 14.09 (13.77) kcal mol^{-1} (Table 1). This TS (TSa, Fig. 1) is used for the following discussion and is the template for all other transition states in this study. Changes in bond length between 1a and its transition state are consistent with the mechanism proposed in Scheme 2. The Se–C and C_α–H bonds are extended by 0.30 (0.25) Å and 0.31 (0.36) Å, respectively (Table 2). The OH bond forming at the transition state is 1.20 (1.16) Å and is coupled to a lengthened Se–O bond. The changing hybridization of C_α and C_β results in a 0.09-Å shortened bond consistent with

Scheme 2 Mechanism of selenoxide elimination from Se-substituted SeCys

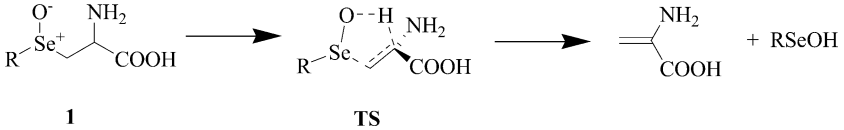

Table 1 Activation energies, reaction energies, and Natural Population Analysis charges for 1a-v and TSa-v at the B3LYP (mPW1PW91) levels

B3LYP							
	R	E_a, kcal mol^{-1}	ΔE_{reac}, kcal mol^{-1}	q_{Se}, 1	q_O, 1	q_{Se}, TS	q_O, TS
a	Me	14.09	3.36	1.383	−1.061	1.061	−0.927
		(13.77)	(8.64)	(1.396)	(−1.069)	(1.090)	(−0.926)
b	Et	13.54	−1.31	1.379	−1.067	1.066	−0.929
		(13.52)	(3.96)	(1.395)	(−1.074)	(1.092)	(−0.926)
c	nPr	13.42	−1.19	1.383	−1.065	1.072	−0.929
		(13.38)	(4.05)	(1.402)	(−1.074)	(1.098)	(−0.925)
d	iPr	13.52	−1.25	1.380	−1.072	1.070	−0.934
		(13.48)	(4.02)	(1.397)	(−1.080)	(1.098)	(−0.931)
e	nBut	13.38	−1.11	1.385	−1.066	1.073	−0.929
		(13.35)	(4.15)	(1.404)	(−1.075)	(1.100)	(−0.926)
f	Bz	14.19	0.01	1.390	−1.060	1.071	−0.927
		(14.18)	(5.25)	(1.390)	(−1.060)	(1.106)	(−0.924)
g	Ph	15.09	−1.72	1.432	−1.069	1.125	−0.930
		(15.32)	(3.67)	(1.446)	(−1.075)	(1.153)	(−0.929)
h	*p*−ClPh	15.03	−2.18	1.442	−1.065	1.129	−0.931
		(15.30)	(3.11)	(1.452)	(−1.073)	(1.159)	(−0.927)
i	*p*-BrPh	15.07	−2.16	1.443	−1.065	1.127	−0.930
		(15.32)	(3.07)	(1.451)	(−1.073)	(1.155)	(−0.925)
j	*p*−IPh	15.06	−2.16	1.443	−1.060	1.130	−0.930
		(15.31)	(3.09)	(1.452)	(−1.073)	(1.156)	(−0.926)
k	*p*-NO_2Ph	15.00	−3.93	1.443	−1.061	1.113	−0.924
		(15.40)	(1.28)	(1.455)	(−1.065)	(1.153)	(−0.921)
l	*p*-MePh	15.00	−1.83	1.435	−1.073	1.128	−0.931
		(15.16)	(3.68)	(1.445)	(−1.077)	(1.156)	(−0.930)
m	*p*-MeOPh	14.59	−2.06	1.438	−1.076	1.135	−0.933
		(14.75)	(3.43)	(1.449)	(−1.078)	(1.163)	(−0.925)
n	*p*-NH_2	14.43	−2.22	1.433	−1.074	1.134	−0.936
		(14.54)	(3.31)	(1.444)	(−1.079)	(1.161)	(−0.929)
o	*o*-ClPh	14.67	−3.36	1.455	−1.069	1.120	−0.939
		(15.04)	(1.81)	(1.465)	(−1.075)	(1.146)	(−0.938)
p	*o*-BrPh	14.63	−3.48	1.453	−1.074	1.120	−0.940
		(14.92)	(1.64)	(1.463)	(−1.077)	(1.147)	(−0.940)
q	*o*-IPh	14.58	−3.60	1.450	−1.073	1.118	−0.942
		(14.88)	(1.54)	(1.461)	(−1.081)	(1.143)	(−0.941)
r	*o*-NO_2Ph	11.92	−10.29	1.478	−1.076	1.168	−0.958
		(12.10)	(−5.23)	(1.497)	(−1.088)	(1.192)	(−0.960)
s	*o*-$PhCH_2NMe_2$	13.37	−7.35	1.444	−1.102	1.162	−0.970
		(13.17)	(−2.55)	(1.455)	(−1.111)	(1.201)	(−0.975)
t	*p*-$PhCH_2NMe_2$	15.41	−2.06	1.436	−1.070	1.127	−0.931
		(15.69)	(3.78)	(1.445)	(−1.072)	(1.153)	(−0.923)
u	*o*-oxazolinePh	13.64	−7.37	1.450	−1.094	1.173	−0.972
		(13.57)	(−2.64)	(1.463)	(−1.104)	(1.209)	(−0.971)
v	*p*-oxazolinePh	15.36	−2.18	1.431	−1.060	1.124	−0.930
		(15.64)	(3.09)	(1.450)	(−1.075)	(1.154)	(−0.925)

double-bond formation. The Natural Population Analysis (NPA) charge for Se decreases by ~0.3 e between 1a and TSa, corresponding to the evolving Se oxidation state [selenoxide (Se^{IV}) to selenenic acid (Se^{II})].

Donation of electron density from larger alkyl groups stabilizes positive charge on Se, leading to lower E_as for selenoxide elimination. The benzyl derivative is similar energetically to 1a. The E_a decreases slightly as the chain length in R increases (Me≈Bz>Et>*n*Pr≈*i*Pr>*n*Bu) for an overall reduction of 0.7 (0.4) kcal mol^{-1} between Me and *n*Bu 1e. The calculated geometries of 1b-f and TSb-f around the selenium center do not change significantly, compared to the methyl derivative, but the changes in bond length for the reaction coordinate show more C_α–H bond

Table 2 Selected B3LYP geometric parameters for 1a-v and TSa-v

	R	Δ(Se–C_R)	Δ(Se–C_β)	Δ(C_α–C_β)	Δ(C_α–H)	1 O–H	TS O–H
a	Me	−0.011	0.299	−0.093	0.314	2.062	1.200
b	Et	−0.009	0.284	−0.091	0.323	2.040	1.193
c	nPr	−0.009	0.281	−0.092	0.325	2.041	1.192
d	iPr	−0.010	0.279	−0.091	0.325	2.024	1.192
e	nBut	−0.010	0.281	−0.092	0.325	2.033	1.192
f	Bz	−0.009	0.289	−0.092	0.325	2.041	1.190
g	Ph	−0.022	0.292	−0.091	0.302	2.071	1.209
h	*p*-ClPh	−0.023	0.302	−0.092	0.295	2.106	1.214
i	*p*-BrPh	−0.023	0.302	−0.092	0.295	2.106	1.215
j	*p*-IPh	−0.023	0.304	−0.092	0.295	2.105	1.215
k	*p*-NO_2Ph	−0.025	0.328	−0.095	0.279	2.129	1.229
l	*p*-MePh	−0.023	0.289	−0.090	0.305	2.074	1.207
m	*p*-MeOPh	−0.023	0.276	−0.088	0.310	2.063	1.203
n	*p*-NH_2	−0.025	0.268	−0.088	0.314	2.055	1.201
o	*o*-ClPh	−0.027	0.345	−0.099	0.279	2.059	1.228
p	*o*-BrPh	−0.027	0.342	−0.099	0.281	2.052	1.228
q	*o*-IPh	−0.027	0.342	−0.100	0.281	2.058	1.227
r	*o*-NO_2Ph	−0.038	0.319	−0.098	0.270	2.042	1.242
s	*o*-$PhCH_2NMe_2$	−0.027	0.248	−0.087	0.293	1.969	1.219
t	*p*-$PhCH_2NMe_2$	−0.023	0.287	−0.091	0.306	2.075	1.206
u	*o*-oxazolinePh	−0.022	0.271	−0.088	0.295	2.080	1.221
v	*p*-oxazolinePh	−0.023	0.299	−0.091	0.297	2.091	1.213

cleavage and less Se–C_β bond cleavage and O–H bond formation as alkyl chain length increases.

The phenyl derivative 1g has a higher E_a than the alkyl derivatives due to π delocalization, which pulls electron density away from Se and reduces the basicity of O_{SeO}. The extent of C_α–C_β bond formation and Se–C_β bond cleavage in TSg are similar to those calculated for TSa (Fig. 1), but the C_α–H distance is slightly shorter in TSg, suggesting that the transition state for the phenyl derivative occurs earlier along the reaction pathway. The decrease in *d*(Se–C_{Ph}) at the transition state results in a shorter distance between an *ortho*-hydrogen and Se (0.13 Å) compared to 1g. This bond contraction will increase the likelihood that *ortho*-substituted groups will influence reactivity at Se.

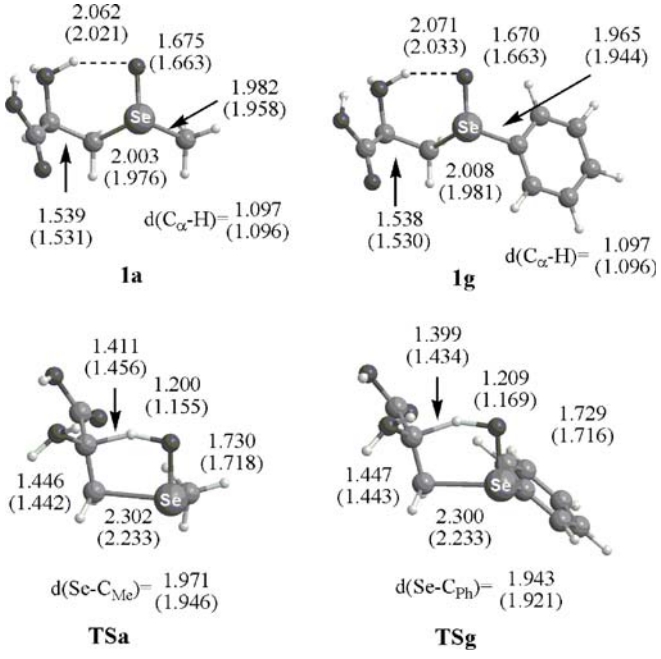

Fig. 1 Selected B3LYP (mPW1PW91) bond distances (Å) for Se-methyl-(1a) and Se-phenylSeCys (1g)

Para substitutions to the ring tend to have little effect upon the activation barrier, regardless of the group's activating or deactivating property. The activation barriers for the halides and the strongly deactivating nitro group are the same as for the unsubstituted phenyl. The activating NH_2 and methoxy-substituted derivatives reduce E_a by ~0.5–0.8 kcal mol^{-1} because the increased charge density in the ring allows more negative charge to reside on the selenoxide oxygen. The NPA charges show little change in electron density at O_{SeO} due to delocalization through hydrogen bonding to the amine, but the activating groups have shorter O_{SeO}–H_{NH} distances (Table 2), corresponding to higher basicity of their selenoxide oxygens. The shortest O_{SeO}–H_{NH} distance belongs to the aniline 1n, the *para*-substituted derivative with the lowest E_a. The values of these parameters suggest that transition states for deactivating substitutents occur earlier than those for activating groups (e.g., *d*(C_α–H=1.376 (1.410) Å for 1k; 1.411 (1.447) Å for 1n). However, an examination of the extent of Se–C_β and C_α–H bond breakage at the TS [ΔE(Se–C_β) and ΔE(C_α–H) in Table 2] shows that while the former is more

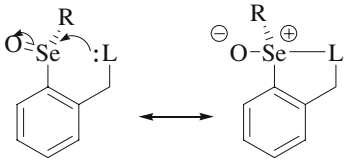

Scheme 3 Resonance structures for interactions between a selenoxide and an ortho-substituted Lewis base donor

prominent for deactivated rings, abstraction of the α-proton is more important for activated rings.

Ortho substitution of certain pendant groups is known to influence the reactivity of GPx mimics and stabilize unstable selenium functionalities. The close proximity of a pendant group in 1g would reduce the barrier to elimination because electron density donated to Se will approximate a three-center-four-electron (3c4e) hypervalent interaction, favoring single Se–O bond character and higher basicity at O_{SeO} (Scheme 3). This interaction will also make the Se group a better leaving group. The effect will be more pronounced than shown in the *para*-substituted derivatives due to the direct donation to Se.

The interactions for the *ortho*-substituted halides 1o-q are weak because the 1,4-interaction does not allow for close contact between Se and X. Nonetheless, a slightly smaller E_a relative to the *para* halides 1h-j was calculated, indicating that donation from the halogen is possible. NBO donor-acceptor energies (Table 3) show that the small interaction between halogen lone pairs and Se–O antibonding orbitals increases as Cl<Br<I and corresponds to a slight reduction in E_a. The small size of Cl allows the closest contact with Se (1h: 3.373 (B3LYP); 3.333 (mPW1PW91); the Se–Cl distance is shorter by ~0.12 Å at the TS (slightly shorter than the *ortho* Se–H_{Ph} distance in 1g). Distances to the larger halogens are longer, 1g (1p: *d* (Se–Br)=3.476 (3.430); TSp: *d*(Se–Br)=3.356 (3.301); 1q: *d*(Se–I)=3.623 (3.570); TSq: *d*(Se–I)=3.499 (3.438)), but the softness of the Br and I atoms and greater interactions between their expansive electron clouds and the selenoxide lead to lower E_a than Cl.

Three additional *ortho*-substituted RSeCys derivatives were included in our study: *Se*-(2-nitrophenyl)SeCys (1r), Se-(2-(*N*,*N*-dimethylamino)methylphenyl)SeCys (1s) and *Se*-(2-oxazolylphenyl)SeCys (1u). Intramolecular Se·O interactions with an *ortho* nitro group allowed the isolation of 2-nitrophenylselenenic acid, the product of selenoxide elimination from 1r [22]. Crystal structures are available for selenenyl halide analogues of 2-(dimethyl)oxazolylphenylselenenic acid [23], but GPx mimics incorporating this pendant group display no GPx-like activity due to the strong Se·N interaction [24]. In comparison, organoselenium compounds of *N*,*N*-dialkylbenzylamine have moderate GPx-like activity [25]. 1u and an analogue of 1s were synthesized by Phadnis and Mugesh. Both were air-stable and 1s showed GPx-like activity superior to ebselen [10].

Ortho substitution of these pendant groups results in the reduction of E_a by ~1.5 kcal mol^{-1} for the nitrogen donors and 3.2 kcal mol^{-1} for 1r (Table 1). Of these three compounds, 1r has the shortest Se–L distance in the reactant state [2.749 (2.712) Å] and the TS [2.604 (2.563) Å] (Fig. 2). Data for *para* substitution of these groups (1k, 1t, 1v) are included in Tables 1 and 2 for comparison. Nitrogen donors generally interact more strongly with Se, but, as we have shown previously, the actual strength depends upon the N,O functionality [14]. In the present comparison, the nitro-oxygens are negatively charged and stabilize TSr more so than the interactions in the nitrogen donors. 1u is predicted to have a similar rate of selenoxide elimination to the RSeCys derivative of a true GPx mimic, even though oxazolyl GPx mimics are inactive due to strong Se···N interactions (1u is not likely to be an active chemopreventative) resulting from aromatic stabilization. This stabilization is not possible for the RSeCys derivatives so that 1s and 1u have similar barriers to selenoxide elimination. The ΔE_{react} values for these compounds are lower than other RSeCys derivatives because Se···N,O interactions stabilize the selenenic acid products.

Conclusions

The above theoretical study shows that inductive effects due to the R group of RSeCys derivatives have little effect upon the activation barrier to selenoxide elimination. Increasing the alkyl chain length lowers E_a by 0.7 (0.4) kcal mol^{-1} vs 1a and translates into a tripling (doubling) of the rate of elimination [k_{1e}/k_{1a}= 3.3 (2.0)]. The rate of selenoxide elimination for aryl RSeCys

Table 3 Natural bond orbital donor–acceptor energies ($\Delta E_{d\to a}$) in kcal mol^{-1} for ortho-substituted phenylselenocysteine

		$\Delta E_{d\to a}$ (B3LYP), kcal mol^{-1}		$\Delta E_{d\to a}$ (mPW1PW91), kcal mol^{-1}	
		1	TS	1	TS
o	*o*-Cl	1.23	2.20	1.41	2.62
p	*o*-Br	1.43	2.52	1.66	3.11
q	*o*-I	1.49	2.72	1.81	3.32
r	*o*-NO_2	4.47	8.88	5.09	10.35
s	*o*-CH_2NMe_2	4.24	6.00	5.17	7.63
u	*o*-oxazolinePh	4.18	6.57	5.09	8.66

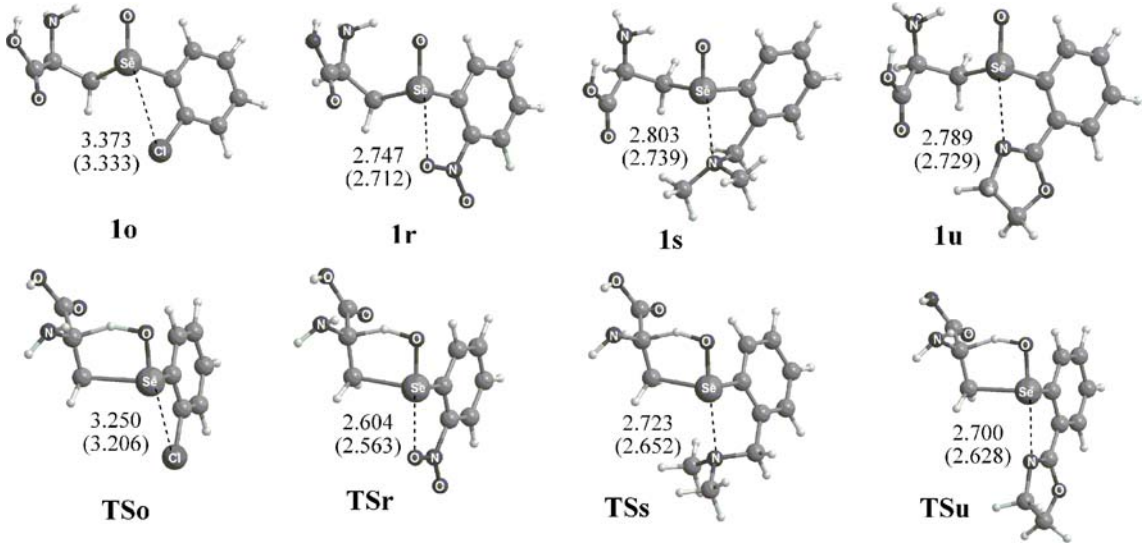

Fig. 2 B3LYP (mPW1PW91) Se–N,O bond distances (Å) for Se-substituted SeCys incorporating *ortho*-pendant groups

derivatives is predicted to be slower than for alkyl derivatives. *Para* activating groups decrease E_a slightly, but only net a 2.3- (1m) or 3.0-fold (1n) rate increase over 1g (B3LYP). A linear relationship (Fig. 3) can be shown between the experimental specific activities for pyruvate formation from RSeCys derivatives in the presence of microsomal oxidases [8] and the E_a values for 1a, 1f, 1g and 1l. This plot suggests that rates of selenoxide elimination can be increased by varying the R group, but the relationship will be valid only if selenoxide elimination is rate-determining.

Direct donation of electron density from an *ortho* donor group has the greatest effect upon E_a. Each of the three pendant groups is predicted to increase the rate of selenoxide elimination by one or two orders of magnitude. The *ortho*-nitro selenoxide 1r is predicted to be especially short-lived with an more than 200-fold rate increase over 1g [k_{1r}/k_{1g}=211 (230)]. The increased stability [12] of these compounds in conjunction with the increased rate of selenoxide elimination may be a useful property for potential prodrugs. Because selenoxide elimination competes with reduction back to the selenide, groups that accelerate elimination will favor formation of selenenic acids that can be reduced to selenols.

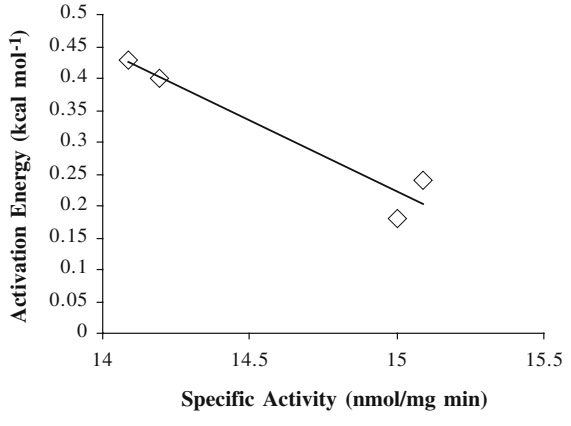

Fig. 3 Plot of the activation energies of 1a, 1f, 1g, and 1l vs the specific activity of pyruvate formation from [6]

Acknowledgements Funding for this project was provided by the Thomas F. Jeffress and Kate Miller Jeffress Memorial Trust.

References

1. Ganther HE, Lawrence JR (1997) Tetrahedron 53:12299–12310
2. (a) Reddy BS, Tanaka T, El-Bayoumi K (1985) J Natl Cancer Inst 74:1325–1328, (b) Tanaka T, Reddy BS, El-Bayoumi K (1985) Jpn J Cancer Res 76:462–467
3. Mugesh G, du Mont WW, Sies H (2001) Chem Rev 101:2125–2179
4. Andreadou I, Menge WMPB, Commandeur JNM, Worthington EA, Vermeulen NPE (1996) J Med Chem 39:2040–2046
5. Rooseboom M, Vermeulen NPE, van Hemert N, Commandeur JNM (2001) Chem Res Toxicol 14:996–1005
6. (a) Commandeur JNM, Andreadou I, Rooseboom M, Out M, de Leur LJ, Groot E, Vermeulen NPE (2000) J Pharmacol Exp Ther 294:753–761, (b) Rooseboom M, Vermeulen NPE, Andreadou I, Commandeur JNM (2000) J Pharmacol Exp Ther 294:762–769
7. Rooseboom M, Commandeur JNM, Floor GC, Rettie AE, Vermeulen NPE (2001) Chem Res Toxicol 14:127–134
8. Andreadou I, van de Water B, Commandeur JNM, Nagelkerke FJ, Vermeulen NPE (1996) Toxicol Appl Pharmacol 141:278–287
9. Musaev DG (2004) J Phys Chem B 108:18756–18761
10. Mugesh G, du Mont WW (2001) Chemistry 7:1365–1370 and references therein
11. Rooseboom M, Schaaf G, Commandeur JNM, Vermeulen NPE, Fink-Gremmels J (2002) J Pharmacol Exp Ther 301:884–892
12. Phadnis PP, Mugesh G (2005) Org Biomol Chem 3:2476–2481

13. (a) Iwaoka M, Tomoda S (1995) J Org Chem 60:5299–5302, (b) Iwaoka M, Tomoda S (1996) J Am Chem Soc 118: 8077–8084, (c) Komatsu H, Iwaoka M, Tomoda S (1999) Chem Commun 205–206, (d) Iwaoka M, Komatsu H, Katsuda T, Tomoda S (2004) J Am Chem Soc 126:5309–5317, (e) Iwaoka M, Komatsu H, Tomoda S (1998) Chem Lett 969–970, (f) Iwaoka M, Komatsu H, Katsuda T, Tomoda S (2002) J Am Chem Soc 124:1902–1909, (g) Iwaoka M, Katsuda T, Tomoda S, Harada J, Ogawa K (2002) Chem Lett 518–519, (h) Iwaoka M, Katsuda T, Komatsu H, Tomoda S (2005) J Org Chem 70:321–327, (i) Bayse CA, Baker RA, Ortwine KN (2005) Inorg Chim Acta 358:3849–3854
14. Ritchey JA, Davis BM, Pleban PA, Bayse CA (2005) Org Biomol Chem 3:4337–4342
15. (a) Becke AD (1993) J Chem Phys 98:5648–5652, (b) Lee C, Yang W, Parr RG (1988) Phys Rev B37:785–789, (c) Colle R, Salvetti O (1975) Theor Chim Acta 37:329–334
16. Adamo C, Barone V (1998) J Chem Phys 108:664–675
17. Frisch MJ, Trucks GW, Schlegel HB, Scuseria GE, Robb MA, Cheeseman JR, Zakrzewski VG, Montgomery Jr JA, Stratmann RE, Burant JC, Dapprich S, Millam JM, Daniels AD, Kudin KN, Strain MC, Farkas O, Tomasi J, Barone V, Cossi M, Cammi R, Mennucci B, Pomelli C, Adamo C, Clifford S, Ochterski J, Petersson GA, Ayala PY, Cui Q, Morokuma K, Malick DK, Rabuck AD, Raghavachari K, Foresman JB, Cioslowski J, Ortiz JV, Baboul AG, Stefanov BB, Liu G, Liashenko A, Piskorz P, Komaromi I, Gomperts R, Martin RL, Fox DJ, Keith T, Al-Laham MA, Peng CY, Nanayakkara A, Gonzalez C, Challacombe M, Gill PMW, Johnson B, Chen W, Wong MW, Andres JL, Gonzalez C, Head-Gordon M, Replogle ES, Pople JA (1998) Gaussian 98, revision A.9. Gaussian, Pittsburgh, Pennsylvania
18. Hurley MM, Pacios LF, Christiansen PA, Ross RB, Ermler WC (1986) J Chem Phys 84:6840–6853
19. Dunning TH (1971) J Chem Phys 55:716–723
20. Dunning TH (1970) J Chem Phys 53:2823–2833
21. Reed AE, Curtiss LA, Weinhold F (1988) Chem Rev 88: 899–926
22. (a) Reich HJ, Willis WW, Wollowitz S (1982) Tetrahedron Lett 23:3319–3322, (b) Kice JL, McAfee F, Slebocka-Tilk H (1982) Tetrahedron Lett 23:3323–3326
23. Mugesh G, Panda A, Singh HB, Butcher RJ (1999) Chem Eur J 5:1411–1421
24. Sarma BK, Mugesh G (2005) J Am Chem Soc 127: 11477–11485
25. (a) Iwaoka M, Tomoda S (1994) J Am Chem Soc 116: 2557–2561, (b) Mugesh G, Panda A, Singh HB, Punekar NS, Butcher RJ (2001) J Am Chem Soc 123:839–850